MICROSTRIP LINE JUNCTIONS

- A Comparison of WIPL-D Simulations and Measured Data

RONALD H. JOHNSTON
UNIVERSITY OF CALGARY
DEPARTMENT OF ELECTRICAL AND COMPUTER ENGINEERING
Calgary, Alberta, Canada
T2N 1N4
Telephone (403) 220-5003
Fax (403) 282-6855
johnston@enel.ucalgary.ca

ABSTRACT

Microstrip line junctions such as corners and Tees are numerically simulated using WIPL-D. The derived scattering parameters are compared with measured and de-embedded scattering parameters of the same junctions. Very good agreement between the simulations and measurements are obtained.

1. INTRODUCTION

The characterization of various microstrip line junctions has received extensive treatment in the literature. Many methods of analysis have been used to determine the S parameters of various microstrip line discontinuities or junctions. Some of the various approaches to the analysis of junctions are: modal analyses [1], 2D equivalent circuits [4,2], the transmission line matrix method [3], spectral domain techniques [4], the moment method with Green's function [5], and assignment of equivalent lumped inductors and capacitors [6,7].

In spite of the availability of many methods, it is clear that a consensus has not been reached on the behavior of given junctions. In fact the discrepancy of the various theoretical models against each other and against measurements can be very substantial. For example, many methods cannot predict radiation from the junction even though it appears that radiation can have a very significant effect on the scattering parameters of the junction.

It is desirable to have available scattering parameters for any microstrip junction in a microstrip of any environment (i.e. any h, any e_r and any Z_0). It is therefore desirable to generalize the scattering parameters of a junction so as to accommodate any microstrip environment. It is even more important to be able to generate the scattering parameters of an arbitrary discontinuity, in an arbitrary microstrip environment, using a numerical EM simulation package.

2. MEASUREMENT METHODS

Measurements on large-scale microstrip transmission line junctions have been conducted with a network analyzer by Johnston and Yang [8]. Two main methods have been used to isolate the junction from the necessary coaxial to microstrip line transitions. In the first method, coax to microstrip transitions are carefully measured and then mathematical extracted from the junction measurements to isolate the S parameters of the junction. In the second method the transmission lines between the coax to microstrip transition and the junction under test are made relatively long and time windowing of time domain measurement data is used to isolate the reflection and transmission behavior of the junction. The remaining data was converted into the frequency domain for presentation as S parameter data.

Careful measurements were made on microstrip corners and Tees with 50 Ω microstrip lines with substrate dielectric constants of 2.55 and 10.0[8]. The S parameters of corners and Tees were presented as a function of normalized frequency, which showed a very close correspondence between the two different microstrip lines.

The normalized frequency is

$$f_{norm} = f_{meas}\ W_e(f)\ \sqrt{\varepsilon_e(f)} \qquad \text{where} \qquad \varepsilon_e = \frac{\varepsilon_r + 1}{2} + \frac{\varepsilon_r - 1}{2} \bullet \left(1 + 12h/w\right)^{-0.5}$$

$$Zo = 120\ \pi \left[\varepsilon_e^{0.5} \bullet \left(\frac{w}{h} + 1.393 + 0.667 \bullet 1n\left(\frac{w}{h} + 1.444\right)\right)\right]^{-1} \qquad W_e = \frac{120\pi h}{Z_o\, \varepsilon_e^{0.5}}$$

$$f_p = \frac{c}{2 W_e\, \varepsilon_e^{0.5}} \qquad f_c = \frac{c}{4h\left(\varepsilon_r - 1\right)^{0.5}}$$

$$\varepsilon_e(f) = \frac{\left[\varepsilon_e \bullet \varepsilon_r \bullet \left[1 + \left(\frac{f}{f_c}\right)^2\right]\right]^2}{\left[\varepsilon_r^{0.5} + \varepsilon_e^{0.5} \bullet \left(\frac{f}{f_c}\right)^2\right]^2} \qquad \text{and} \qquad W_e(f) = w + \frac{\left(W_e - w\right)}{1 + \left(\frac{f}{f_p}\right)^2}\ .$$

The measured scattering parameters of the corners are shown in Figures 1 and 2 and the scattering parameters of the Tees are shown in Figures 3, 4, 5, and 6. In these plots the S parameters are plotted as a function of normalized frequency.

3. NUMERICAL SIMULATION METHOD

Much the same challenge exists for using WIPL-D to determine the S parameters of a microstrip line junction as occurs in measuring a physical microstrip junction. It is necessary to launch a wave on to the microstrip line (of selected dimensions) without creating artifacts from the wave launching structure and wave recovery structure. This problem is overcome by tapering the microstrip line height and width to very small dimensions and thereby removing high frequency effects that can occur at the wave launch and recovery structures (i.e. the input and output transitions from microstrip to input and output ports). The constructed tapered lines should be tested using a straight section of line and the dimensions of the launchers may be adjusted to maximize S_{21} and minimize S_{11}. See Figure 7. The scattering parameters of the straight section with tapered transitions are shown in Figure 8. The low value of S_{11} and high value of S_{21} was achieved by adjusting the diameter of the feed wires, the taper length and the width of the microstrip line where it is attached to the wires and the height of the dielectric at the feed edges. The taper length (LT) is 10 mm, substrate height (h) is 3.17 (or 6.34) mm, the reduced substrate height is h1, the length of line from taper to the centre axis of the junction is L1 (usually 20 mm) and the distance from the centre axis of the corner to the outside edge of the substrate is L4 (usually 20 mm). The width of the narrow end of the tapered microstrip line is wa. Ideally $|S_{21}|$ would have a value of 1.0 for all frequencies and $|S_{11}|$ would have a value of 0.0 for all frequencies. The magnitudes of S_{21} and S_{11} suggest that the transitions approach but do not achieve perfect transition behavior and it also appears that some radiation occurs from the structure. In general the S parameter plots tend to show some evidence of small multiple reflections between the transitions and the junction. Small adjustments are normally made to the transition dimensions to minimize the ripple due to multiple reflections. To obtain the most consistent results the WIPL-D options "integral accuracy-enhanced 1" and "current expansion-enhanced 1" are used.

4. SIMULATION RESULTS

After satisfactory transitions have been constructed, the other junctions may be constructed and simulated using WIPL-D. See Figure 9 for the construction of the right angle corner. This structure has been analyzed for 50 Ω lines on a substrate with dielectric constants of 2.55 and 10.0. The scattering parameters for the corners are shown in Figures 10 and 11 for the two respective dielectric substrates. The results of the S parameters of these two lines are plotted using the normalized frequency described earlier and are plotted in Figures 12 and 13 along with measured S parameter data as per Ref. 8. It will be noted that the agreement between the WIPL-D generated S parameters and the measured S parameters is very good up to high frequencies.

It was noted, while doing the simulations, that the peak value of $|S_{11}|$ was dependent on the distance from the corners to the edge of the substrate. The peak value generally decreased as the distance to the edge increased. This in turn suggests that radiation from the corner increased especially at frequencies where $|S_{21}|$ was going to low values.

The construction of the microstrip Tee is shown in Figure 14. The simulated S parameters of the $\varepsilon_r = 2.55$ substrate microstrip Tee are shown in Figure 15. The simulated S parameters of the $\varepsilon_r = 10$ substrate microstrip Tee are shown in Figure 16. The individual S parameters for the simulated Tees and the measured Tees are plotted in Figures 17 to 20 as a function of normalized frequency. In each figure: the heavy solid line is measured data where $\varepsilon_r = 2.55$, the heavy dashed line is measured data where $\varepsilon_r = 10$, the light dash dot line is simulated data where $\varepsilon_r = 2.55$ and the light dashed line is simulated data where $\varepsilon_r = 10$. Figure 17 shows $|S_{11}|$ measured and simulated data, Figures 18 and 19 show $|S_{21}|$ and $|S_{31}|$ measured and simulated data respectively. Figure 20 shows $|S_{33}|$ measured and simulated data.

In general the agreement between the measured and simulated results are very good, especially where $\varepsilon_r = 2.55$. At the higher frequencies there is some deviation between the $|S_{31}|$ and $|S_{33}|$ data for the simulated $\varepsilon_r = 10.0$ the measured $\varepsilon_r = 10$ and the measured $\varepsilon_r = 2.55$ cases.

5. RADIATION

It is evident a significant fraction of the energy incident on the junction will be radiated. It is well known that for a lossless and radiationless two port that:

$$|S_{11}^2| + |S_{21}^2| = 1.0$$

and for a lossless and radiationless three port that:

$$|S_{11}^2| + |S_{21}^2| + |S_{31}^2| = 1.0 \qquad \text{and} \qquad |S_{33}^2| + |S_{32}^2| + |S_{31}^2| = 1.0$$

Due to the symmetry of the microstrip Tee, S_{13} equals S_{23}, and the third equation is not required for the three port.

In examining Figures 11 and 12, one must conclude that in the microstrip corner that one half of the incident energy or more is radiated at normalized frequencies higher than 11 GHz cm. It was found from the simulations that the peak S_{11} became lower as more substrate was added to the outside of the corner and thereby increasing radiation. A radiation pattern was produced using WIPL-D as shown in Figure 21. The radiation pattern tended to change shape fairly rapidly as frequency was changed.

In examining Figures 19 and 20, one can conclude that in the microstrip Tee, if one feeds energy into port 3, that one half or more the incident energy is radiated at normalized frequencies higher than about 12 GHz cm. The peak value of S_{33} decreased as more substrate was added to the top of the Tee thereby increasing radiation. The radiation pattern is shown in Figure 22. It is notable that if the energy is directed into the Tee from port 1 that less radiation will occur. In that case, as the frequency goes up more energy is conveyed into port 2 and port 3 is partially disconnected.

CONCLUSIONS

It is clear that WIPL-D simulations of microstrip junctions can provide very useful information on the corner and Tee junctions. The business of isolating the junction's effects from the effects of other necessary structures (such as wave launchers) presents some difficulty in both physical measurements and numerical simulations. However, if care is taken to do this, then useful knowledge and data can be obtained on microstrip transmission line junctions and discontinuities.

ACKNOWLEDGEMENTS

This research is supported by the Natural Sciences and Engineering Research Council of Canada under grant No. A7701. Dr. Kolundzija's assistance on this project is greatly appreciated.

REFERENCES

1. I. Wolff, G. Kompa and R. Mehran, *"Calculation Method for Microstrip Discontinuities and T-junctions"*, Electron Lett., Vol. 8, pp. 177, April, 1972.
2. R.J. Johnston, D.A. Graham, *"The Frequency Dependence of Microstrip Junction Scattering Parameters"*, Digest of the 27 Midwest Symposium on Circuits and Systems, Morgantown, West Virginia, June, 1984.
3. W.J.R. Hoefer, *"The Transmission-Line Matrix Method – Theory and Applications"*, IEEE Trans. Microwave Theory Tech., Vol. MTT-33, pp. 882-893, October, 1985.
4. R.H. Jansen, *"The Spectral Domain Approach for Microwave Integrated Circuits"*, IEEE Trans. Microwave Theory Tech., Vol. MTT-33, pp. 1043-1056, October, 1985.
5. P.B. Katehi and N.G. Alexopoulos, *"Frequency-dependent Characteristics of Microstrip Discontinuities in Millimeter Wave Integrated Circuits"*, Vol. MTT-33, pp. 1029-1035, October, 1985.
6. P. Silvester and P. Benedek, *"Microstrip Discontinuity Capacitances for Right-Angled Bends, T-junctions and Crossings"*, IEEE Trans. Microwave Theory Tech, Vol. MTT-21, pp. 34-346, May, 1973, (Correction Vol. MTT-23, p. 456, May 1975).
7. A.F. Thomson and A. Gopinath, *"Calculation of Microstrip Discontinuity Inductances"*, IEEE Trans. Microwave Theory Tech., Vol. MTT-23, pp. 648-655, August, 1975.
8. R.H. Johnston and M. Yang, *"A Comparison of Microstrip Discontinuity Models with Measured Data"*, Proceedings of the 35th Midwest Symposium on Circuits and Systems, pp. 9-12, Washington D.C., August, 1992.

FIGURES

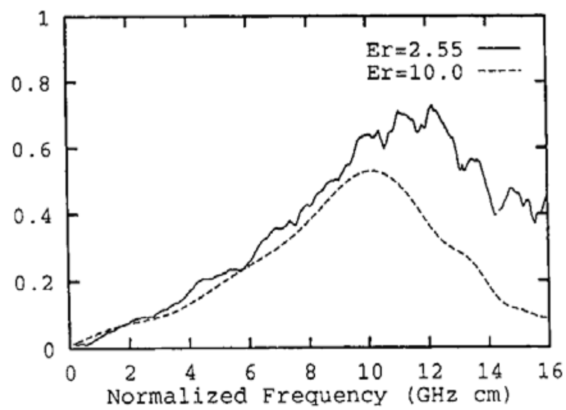

Figure 1: Measured S_{11} of 50 Ω microstrip corners on two different substrates as per Ref. 8.

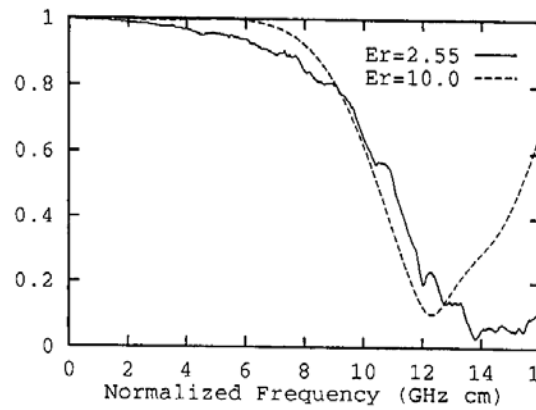

Figure 2: Measured S_{21} of 50 Ω microstrip corners on two different substrates as per Ref. 8.

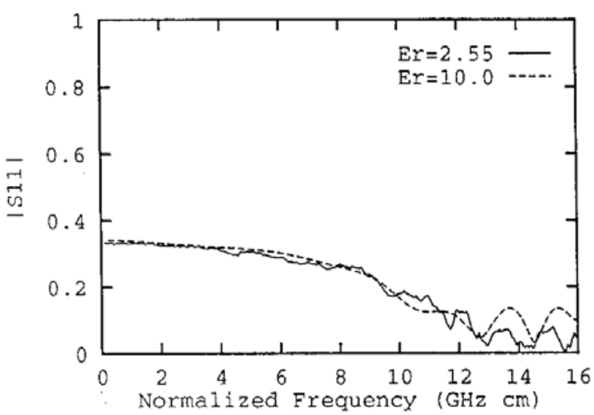

Figure 3: Measured S_{11} of 50 Ω microstrip Tees on two different substrates as per Ref. 8.

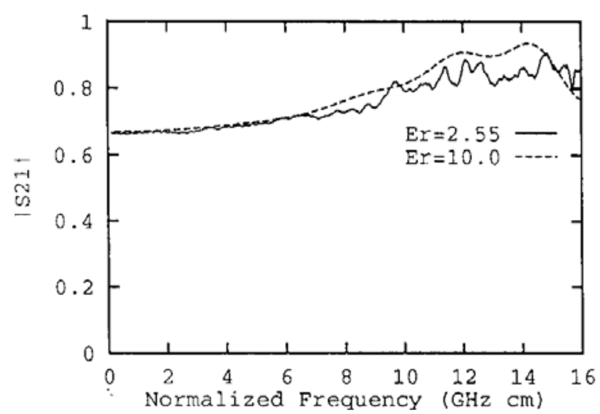

Figure 4: Measured S_{21} of 50 Ω microstrip Tees on two different substrates as per Ref. 8.

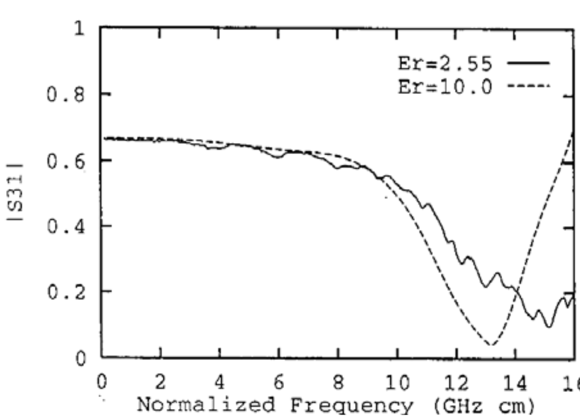

Figure 5: Measured S_{31} of 50 Ω microstrip Tees on two different substrates as per Ref. 8.

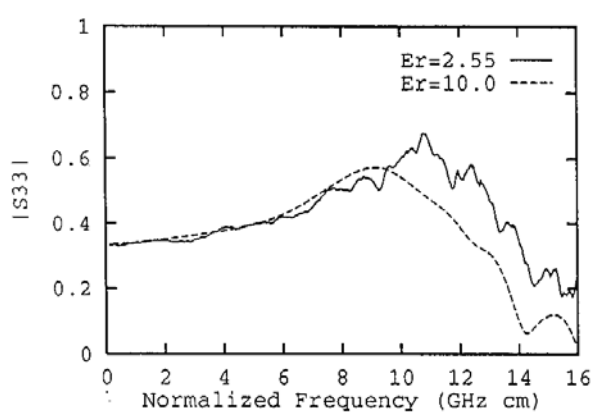

Figure 6: Measured S_{33} of 50 Ω microstrip Tees on two different substrates as per Ref. 8.

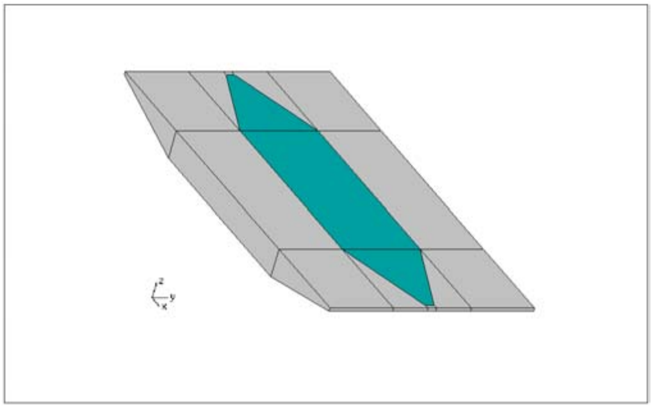

Figure 7: A straight microstrip transmission line with tapered heights at each end. Wires connect the outer ends of the tapered upper connector to the ground plane and to the sources.

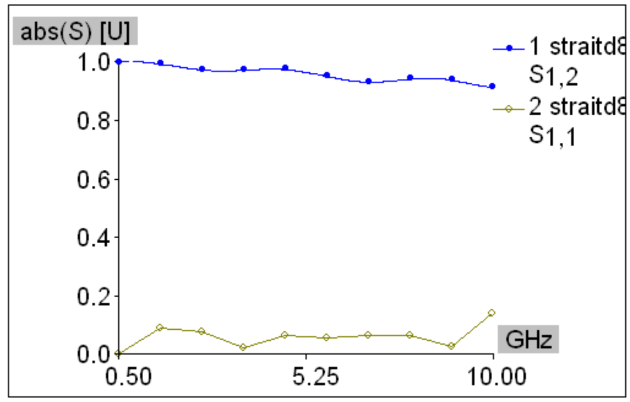

Figure 8: The scattering parameters of the straight microstrip, the two tapers and the connecting wires.

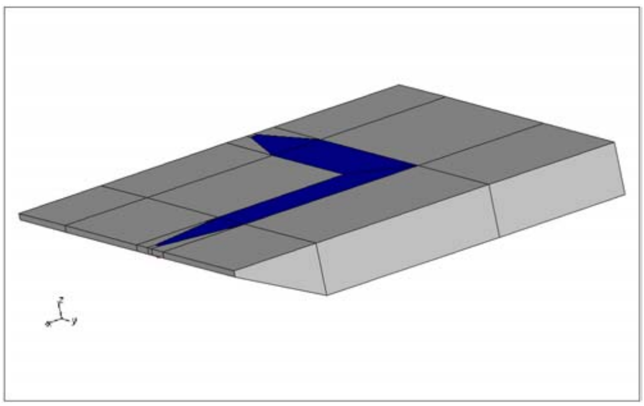

Figure 9: The microstrip corner as simulated with WIPL-D.

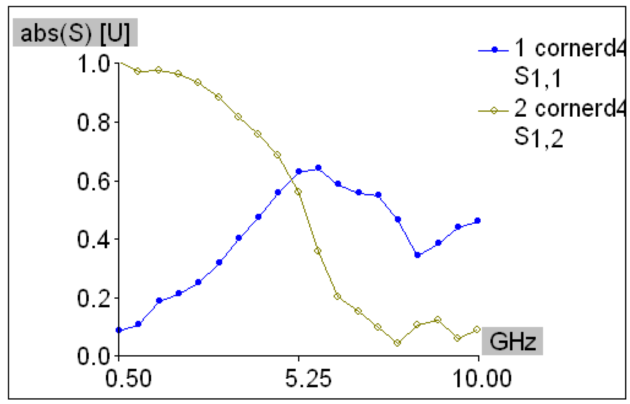

Figure 10: The WIPL-D simulated scattering parameters of the microstrip corner built on the $\varepsilon_r = 2.55$ substrate. $w = 9.1\,mm$, $h = 3.17\,mm$

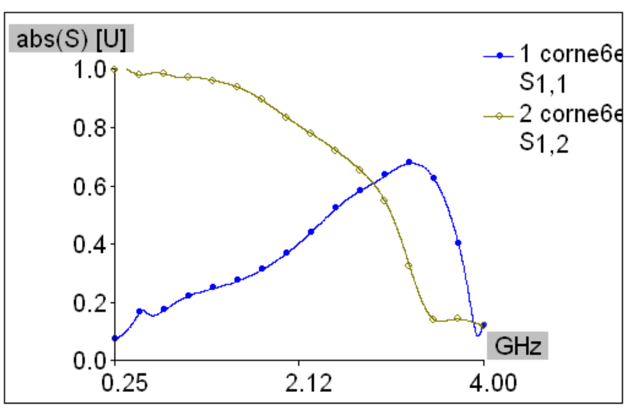

Figure 11: The WIPL-D simulated scattering parameters of the microstrip corner built on the $\varepsilon_r = 10.0$ substrate. $w = 6.34\,mm$, $h = 6.34\,mm$

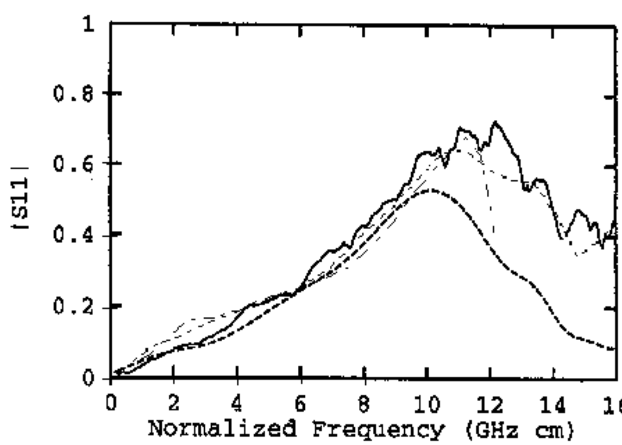

Figure 12: The measured and simulated S_{11} of the corners on the two substrates plotted against normalized frequency. The heavy solid line is $\varepsilon_r = 2.55$, measured. The heavy dashed line is $\varepsilon_r = 10$, measured. The light dotted line is $\varepsilon_r = 2.55$, simulated. The dash dot line is $\varepsilon_r = 10$, simulated.

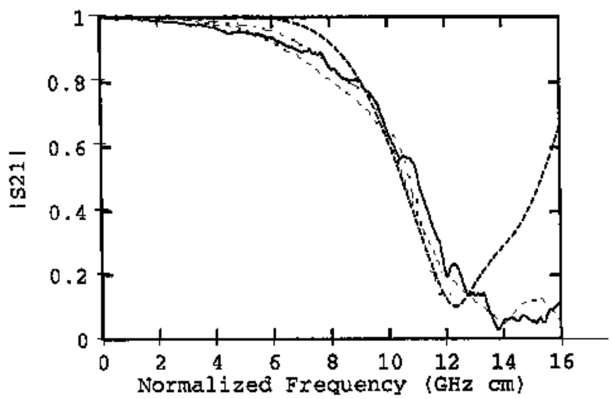

Figure 13: The measured and simulated S21 of the corners on the two substrates plotted against normalized frequency. The heavy solid line is $\varepsilon_r = 2.55$, measured. The heavy dashed line is $\varepsilon_r = 10$, measured. The light dotted line is $\varepsilon_r = 2.55$, simulated. The dash dot line is $\varepsilon_r = 10$, simulated.

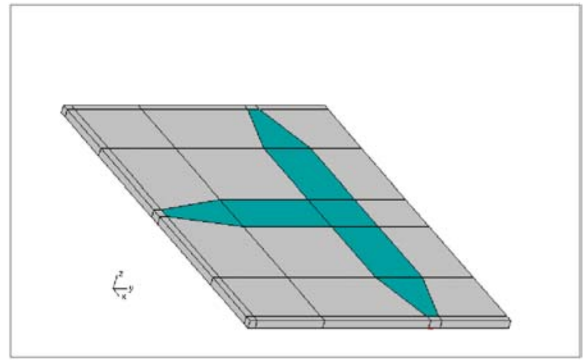

Figure 14: The microstrip Tee as simulated with WIPL-D. Ports 1 and 2 lie on the x-axis. Port 3 lies on the negative y-axis.

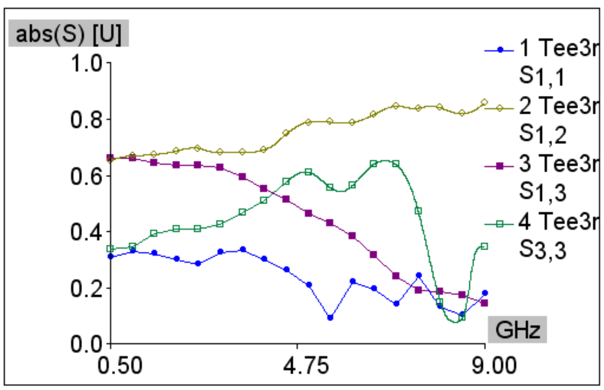

Figure 15: The WIPL-D simulated scattering parameters of the microstrip Tee built on the $\varepsilon_r = 2.55$ substrate, $w = 9.1\,mm$, $h = 3.17\,mm$.

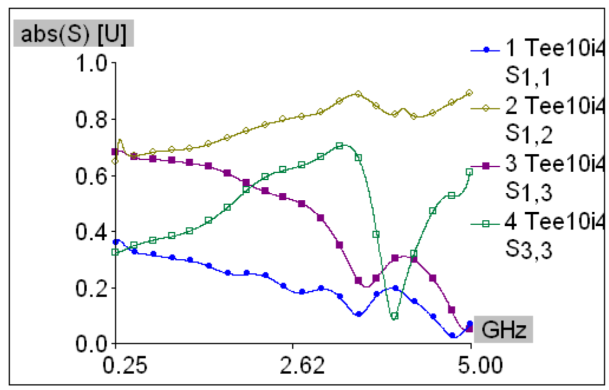

Figure 16: The WIPL-D simulated scattering parameter of the microstrip Tee built on the $\varepsilon_r = 10.0$ substrate, $w = 6.34\,mm$, $h = 6.34\,mm$.

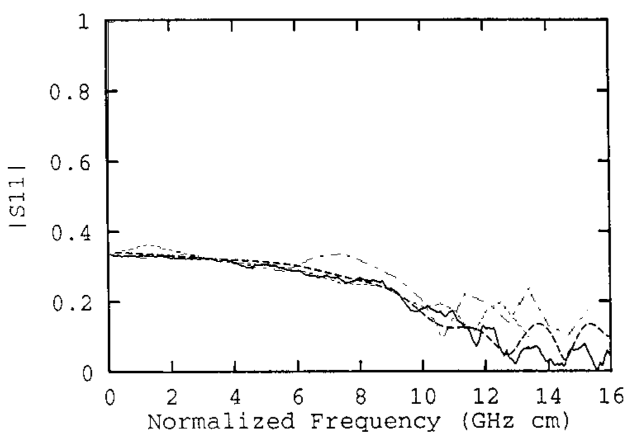

Figure 17: Magnitude of S_{11} of the measured and simulated Tees.

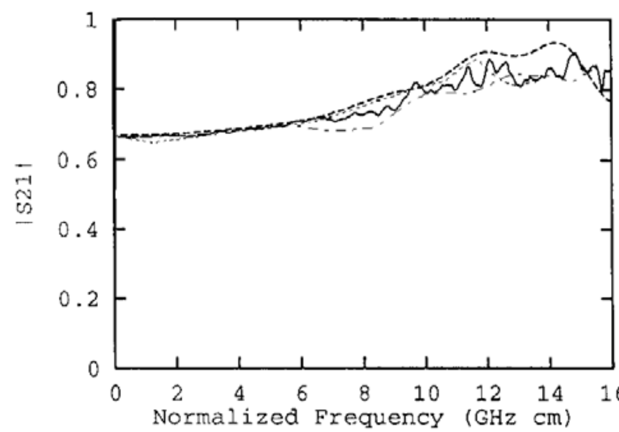

Figure 18: Magnitude of S_{21} of the measured and simulated Tees.

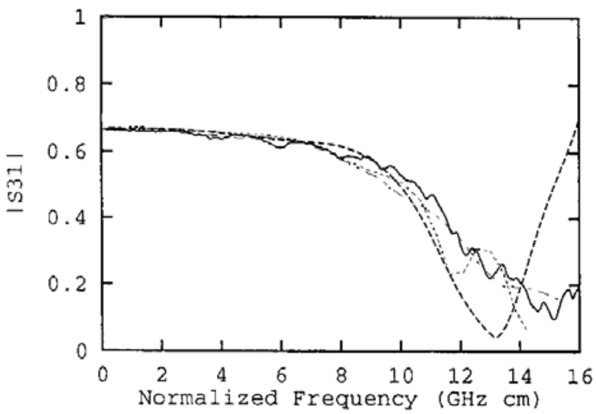

Figure 19: Magnitude of S_{31} of the measured and simulated Tees.

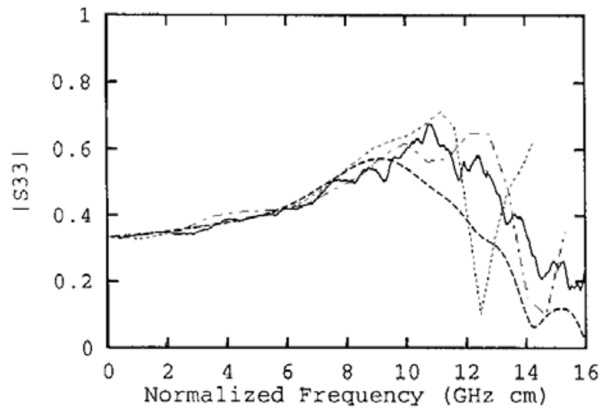

Figure 20: Magnitude of S_{33} of the measured and simulated Tees.

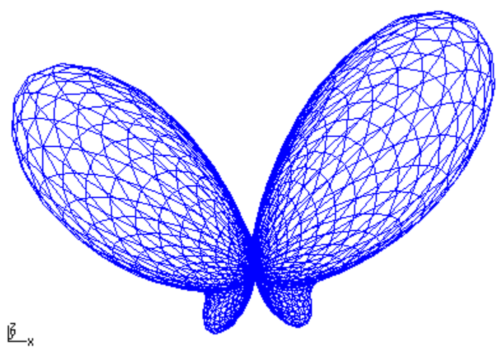

Figure 21: Radiation pattern of the corner built on the $\varepsilon_r = 2.55$ substrate at 6.0 GHz.

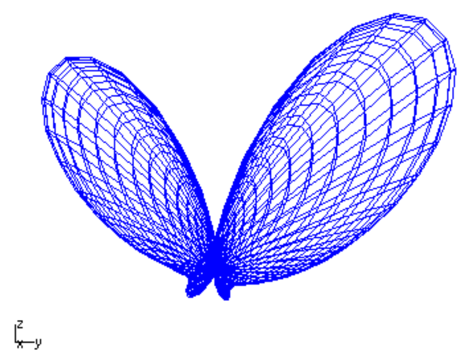

Figure 22: Radiation pattern of the Tee when port 3 is fed on the $\varepsilon_r = 2.55$ substrate at 6.0 GHz.

